Advances in Concrete Construction, *Vol. 15, No. 3 (2023) 161-170*
https://doi.org/10.12989/acc.2023.15.3.161

Effect of fiber content on the performance of UHPC slabs under impact loading – experimental and analytical investigation

Muhammad Umar Khan [1,2a], Shamsad Ahmad*[1,3], Mohammed A. Al-Osta [1,3b], Ali Husain Algadhib [1,3c] and Husain Jubran Al-Gahtani [1,3d]

[1] *Department of Civil & Env. Eng., KFUPM, Dhahran 31261, Saudi Arabia*
[2] *Department of Civil Engineering & Technology, Qurtuba University of Science and Information Technology, D.I. Khan 29150, Pakistan*
[3] *Interdisciplinary Research Center for Construction and Building Materials, KFUPM, Dhahran 31261, Saudi Arabia*

(*Received January 15, 2022, Revised December 12, 2022, Accepted February 22, 2023*)

Abstract. Ultra-high-performance concrete (UHPC) is produced using high amount of cementitious materials, very low water/cementitious materials ratio, fine-sized fillers, and steel fibers. Due to the dense microstructure of UHPC, it possesses very high strength, elasticity, and durability. Besides that, the UHPC exhibits high ductility and fracture toughness due to presence of fibers in its matrix. While the high ductility of UHPC allows it to undergo high strain/deflection before failure, the high fracture toughness of UHPC greatly enhances its capacity to absorb impact energy without allowing the formation of severe cracking or penetration by the impactor. These advantages with UHPC make it a suitable material for construction of the structural members subjected to special loading conditions. In this research work, the UHPC mixtures having three different dosages of steel fibers (2%, 4% and 6% by weight corresponding to 0.67%, 1.33% and 2% by volume) were characterized in terms of their mechanical properties including facture toughness, before using these concrete mixtures for casting the slab specimens, which were tested under high-energy impact loading with the help of a drop-weight impact test setup. The effect of fiber content on the impact energy absorption capacity and central deflection of the slab specimens were investigated and the equations correlating fiber content with the energy absorption capacity and central deflection were obtained with high degrees of fit. Finite element modeling (FEM) was performed to simulate the behavior of the slabs under impact loading. The FEM results were found to be in good agreement with their corresponding experimentally generated results.

Keywords: concrete damage plasticity model; fiber content; finite element modeling (FEM); fracture toughness; impact; UHPC

1. Introduction

A structural member made of reinforced concrete is subjected to various types of loads during its service life, including dead and live gravity loads, seismic forces, impact loads exerted accidentally, and in recent years an increased threat of blast loads from terrorists' attacks (Li *et al*. 2016). These loading conditions might result into flexural and shear damages leading to severe cracking and spalling of concrete (Li *et al*. 2015a). Strategic buildings such as military structures, nuclear power plants, etc., are designed to resist blast and impact loads. In the actual design of nuclear power plants, the containment building should prevent scabbing and perforation under the impact of an aircraft crash (Thai and Kim 2016). Over the years, researchers have been studying the behavior of reinforced concrete members under impact loads (Batarlar 2013, Elavenil and Knight 2012). Concrete, being a brittle material, possesses limited tensile strength and fracture toughness (Azad *et al*. 2012). Therefore, in order to improve the tensile/flexural strength, ductility, and fracture toughness, short-length fibers have been used in the concrete matrix (Yanni 2009). Huang *et al*. (2021) studied the effect of fiber orientation on improving the dynamic properties of UHPC under impact loading by using Spilt Hopkinson Pressure Bar test method. They recorded highest dynamic properties when the fiber orientation was predominantly perpendicular to dynamic loading. In normal concrete construction, compressive strength is considered as an index property and the indicator of the overall quality without much importance given to the toughness and resistance against crack initiation and propagation. Whereas, in ultra-high-performance concrete (UHPC) containing fibers, impact resistance due to high fracture toughness is considered to be equally important as its strength and durability parameters (Elavenil and Knight 2012, Máca *et al*. 2014).

The robustness of UHPC, in terms of its excellent resistance to different loading conditions and resistance against severe aggressive exposure conditions, has been reported due to its dense microstructure. UHPC consists of negligible porosity and extremely low diffusion coefficient

*Corresponding author, Ph.D., Professor,
E-mail: shamsad@kfupm.edu.sa
[a] Ph.D., Assistant Professor
[b] Ph.D., Associate Professor
[c] Ph.D., Associate Professor
[d] Ph.D., Professor

ISSN: 2287-5301 (Print), 2287-531X (Online)

(Filho *et al*. 2012). The dense microstructure and very low porosity resist the ingress of harmful species to give better performance in durability (Farnam *et al*. 2010, Li *et al*. 2016, Máca *et al*. 2014, Othman and Marzouk 2018). Several studies reported the outstanding mechanical and durability properties of UHPC. Kang (2020) demonstrated the impact of using river sand and particle size on the fresh and mechanical properties of UHPC. Tang (2021) studied the effect of mix design and age on the mechanical properties of UHPC. Dadmand *et al*. (2020) investigated the effect of hybrid macro-micro steel and macro steel-polypropylene fibers on the performance of UHPC. Having excellent performance, UHPC is adopted for the construction of containment buildings in nuclear power plants in particular and for fortification structures in the military and other structural applications in general. The higher fracture toughness ensuring greater impact energy absorption of UHPC gives a greater resistance to impact loading and spalling of concrete.

Researchers have been investigating the benefits of incorporating steel fibers in concrete that include enhancements in the tensile strength and energy dissipation characteristics of the concrete. Different tests have been reported in the literature that are used to assess the impact resistance of the concrete containing fibers, such as: i) explosive test; ii) projectile impact test; iii) drop-weight impact test; and iv) Charpy impact test. There is no standardized test to assess the impact resistance. However, the American Concrete Institute (ACI) has suggested drop-weight impact testing for fiber-reinforced concrete members (Elavenil and Knight 2012).

Elavenil and Knight (2012) studied the dynamic behavior (using maximum impact energy of 900 J) of conventional concrete plates reinforced with fibers and subjected to impact loading. They varied the thickness of slabs, fiber content and aspect ratios of fibers. They observed a significant reduction in the width of the developed cracks in the specimens prepared incorporating fibers as compared to that in the specimens prepared without fibers. The reduction in the crack width was more pronounced in the specimens that had steel fibers with higher aspect ratios (i.e., length to diameter ratios). Although this study showed the beneficial effects of the presence of fibers in concrete against cracking under impact loading, the work did not include the information regarding mechanical properties (strength, elasticity, fracture toughness) of the concrete used. Furthermore, their study on the effect of the impact loading on the slabs was limited to low impact energy of 900 J only because the class of the concrete used did not belong to the ultra-high-performance concrete.

Máca *et al*. (2014) investigated the effect of projectile impact resulting in the energy of about 2000 J (using low-weight grains of 8.04 g that hit the concrete at a very high velocity of 710 m/s) on ultra-high-performance fiber-reinforced concrete mixtures with varying fiber contents. They evaluated the effect of the impact in terms of average crater diameter, penetration depth, spalling and scabbing of the slab specimens. They observed that the fiber content beyond 1% and 2% (by volume) is not beneficial in reducing the penetration depth and crater diameter, respectively. They recommended an optimal dosage of fiber content as 2% (by volume) for producing the ultra-high-performance fiber-reinforced concrete mixtures having optimum workability, mechanical properties, and resistance against impact exerted by the projectile.

Farnam *et al*. (2010) evaluated the performance of high-strength fiber-reinforced concrete against impact loading exerted on the slab specimens using a drop-weight impact-testing setup. Concrete mixture containing 2% fibers (by volume) had a compressive strength of 96 MPa. The maximum impact energy (applied by dropping a projectile of 8.5 kg from a height of 1 m several times), corresponding to failure, was less than 500 J. They found impact resistance of concrete mixture with fibers more than that of the mixture without fibers. Their numerically obtained results pertaining to number of blows required for initiation of failure, the shape of failure pattern, the upper and lower diameters of the truncated cone formed due to the damage, and the midpoint deflection (using finite element analysis) were in agreement with the corresponding experimental results.

Li *et al*. (2015b) performed an experimental program on UHPC and normal concrete slabs. It was reported that the slab with normal concrete failed completely when subjected to blast loading whereas the UHPC slab with a similar reinforcement ratio experienced plastic deformation but remained intact, even under higher blast intensity.

Thai and Kim (2016) performed finite element analysis to model the local damage of fiber-reinforced UHPC wall caused by the impact of aircraft engine missiles. The concrete damage plasticity (CDP) model was used to capture the complete behavior of UHPC materials. It is reported that the CDP model is mostly used for the simulation of concrete (Kota *et al*. 2019, Krishna *et al*. 2019, Raza and Ahmad 2020). CDP model was initially introduced for monotonic loading by Lubliner (1989). Lee and Fenves (1998) adopted the CDP model for the cyclic and dynamic loadings applied on the panels made of UHPC. They formulated the CDP model based on the information reported in the literature (Lubliner 1989, Lee and Fenves 1998, Nuclear Energy Institute 2011, Dassault Systèmes Simulia 2016). The numerical results were then compared with the experimental data produced by Riedel *et al*. (2010), based on the parametric studies performed numerically with varying panel thickness, fiber content and impact velocities. The numerical results showed fair agreement with the experimentally obtained data.

The review of the previous studies, as briefly presented above, indicates that many researchers have attempted to study the resistance of the fiber-reinforced concrete against impact loading. However, these studies have considered low levels of impact energy mainly because of the relatively lower grades of fiber-reinforced concrete mixtures used for the experimental investigation. Towards an effort to produce a UHPC that can survive the impact of high intensities, the present work considered the UHPC mixture with varying fiber contents that showed a maximum compressive strength up to 166 MPa and sustained impact energy of as high as 6397 J. The effect of fiber content on the impact

resistance of UHPC slabs was studied experimentally and numerically.

2. Experimental program

UHPC mixtures containing three different percentages of steel fibers were considered in the present study. For comparison purposes, a mixture of high-strength conventional concrete (HSCC) without fibers was also considered. The experimental program was divided into two parts. The first part consisted of preparing and testing the specimens of UHPC and HSCC mixtures for their characterization in terms of compressive strength, modulus of elasticity, flexural tensile strength, direct tensile strength (dog-bone test), and fracture toughness. The slab specimens prepared using UHPC and HSCC mixtures were tested under impact loading in the second part of the experimental program.

2.1 Materials

2.1.1 Binders and fine filler

Type I ordinary Portland cement, conforming to ASTM C150 (ASTM C150-19 2019), was used as the main binder. Silica fume was used as supplementary cementitious material and also to serve as an ultra-fine filler. Another fine material, hematite powder, was also used as filler by replacing 10% of sand (used as main filler in UHPC). The specific gravities of ordinary Portland cement, silica fume and hematite powder were determined as 3.14, 2.33 and 4.98, respectively. The chemical compositions of the silica fume and hematite powder were determined using X-ray fluorescence. Silica fume had 92.13 % of SiO_2 and the hematite powder contained 91.49 % of Fe_2O_3. Further, BET (Brunauer, Emmett and Teller) analysis was performed to determine the specific surface area and average particle size of OPC, SF and HP. The specific surface areas were 0.37, 14.71 and 20.73 m^2/g and average particle sizes were 8.65, 0.40 and 0.289 μm for OPC, SF and HP, respectively.

Table 1 IDs and description of the mixtures

UHPC Mixture ID	Fiber content (% by mass)	Fiber content (% by volume)
M-FC2	2	0.67
M-FC4	4	1.33
M-FC6	6	2.00

2.1.2 Aggregate

Coarse aggregates confirming to ASTM C33 (ASTM C33-18, 2019), No. 7, having a bulk specific gravity of 2.45 and water absorption of 2.05%, were used for the HSCC mixture only. Desert sand comprising of fine quartz with a bulk specific gravity of 2.65 and water absorption of 0.6% was used as fine aggregate in the HSCC mixture and the same sand was used as sole aggregate in the UHPC mixtures.

2.1.3 Superplasticizer (SP)

Glenium 51, conforming to ASTM C494 (ASTM C494-19 2019), was used as a superplasticizer to maintain the required flow for satisfying self-compacting concrete requirements.

2.1.4 Steel fibers

Copper-coated plain steel fibers, having a tensile strength of 2500 MPa and an aspect ratio of 65, were used in the UHPC mixtures. Fibers had a length of 12.7 mm and a diameter of 0.15 mm.

2.2 Details of the HSCC and UHPC mixtures

As mentioned earlier, for studying the effect of fiber content, the UHPC mixtures were prepared to incorporate 2, 4, and 6% of steel fibers (by mass). All these UHPC mixtures had the same amounts of cement, silica fume, superplasticizer, and water. The mixture IDs and their corresponding descriptions are given in Table 1. All the mixtures were proportioned using the absolute-volume equation. One cubic meter of the HSCC mixture contained 150 kg water, 375 kg cement, 728 kg sand, 1092 kg coarse aggregates, and 5.3 kg superplasticizer. The amounts of the ingredients determined for preparing a unit volume of UHPC mixtures are presented in Table 2. All three mixtures had almost the same values of flow (180 to 185 mm), satisfying the workability requirement of a UHPC mixture.

2.3 Casting and curing of specimens

While the HSCC mixture was mixed in a revolving drum mixer, a planetary mixer was used to mix the UHPC mixtures. Soon after the mixture was prepared, it was tested for measuring the flow using the flow table test. The specimens for different tests were cast in the first 30 minutes of the completion of mixing to avoid the loss of moisture. The molds filled with concrete were placed on a vibrating table for compaction. Fig. 1 shows a slab being compacted on a vibrating table. After 24 h of casting, the specimens were demolded and water-cured for a period of 28 days before conducting tests on them.

Table 2 The amount of ingredients for one cubic meter of UHPC mixtures

Mixture ID	Cement (kg)	Silica fume (kg)	SP (kg)	Water (kg)	Sand (kg)	Hematite powder (kg)	Fiber (kg)
M-FC2					929	208	50
M-FC4	900	220	40	157	915	204	100
M-FC6					901	201	150

Fig. 1 Casting of the concrete specimens

2.4 Tests for determining basic mechanical properties

The compressive strength and modulus of elasticity tests were carried out as per ASTM C39 (ASTM C39-18 2018) and ASTM C469 (ASTM C469-14 2014), respectively, using the cylindrical specimens having standard size (75 mm in diameter and the pre-end preparation length of 150 mm). The specimens were loaded at a rate of 1.5 kN/s, and the deformation of the specimens was recorded using LVDTs attached to the specimens. Four-point flexural loading was applied at a rate of 0.5 mm/min on the prism specimens having 40 × 40 × 160 mm size conforming to ASTM C78 (ASTM C78-18 2018). The mid-span deflection was recorded using LVDT attached to the specimens. Dog-bone-shaped specimens were tested to determine the direct tensile strength and the tension damage parameters, which were used in the concrete damaged plasticity model in FEM. Similarly, the compression damage parameters were extracted from the curves obtained from the modulus of elasticity test. The test setups for evaluating the mechanical properties are shown in Fig. 2.

2.5 Impact test on slab specimens

A tailor-made setup for impact testing on slab specimens was designed and fabricated. The square slabs (750 mm × 750 mm × 50 mm) having a clear span of 610 mm were clamped over a steel frame, which was raised above the ground level for installing the LVDT's to monitor the deflections. LVDT's were placed under the slab at ten pre-determined critical locations to measure the deflections induced by the impact loads, as shown in Fig. 3.

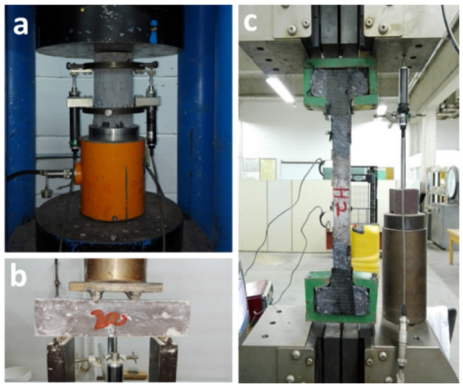

Fig. 2 (a) Compressive strength and modulus of elasticity; (b) flexural strength; and (c) dog-bone specimen for direct tension test setups

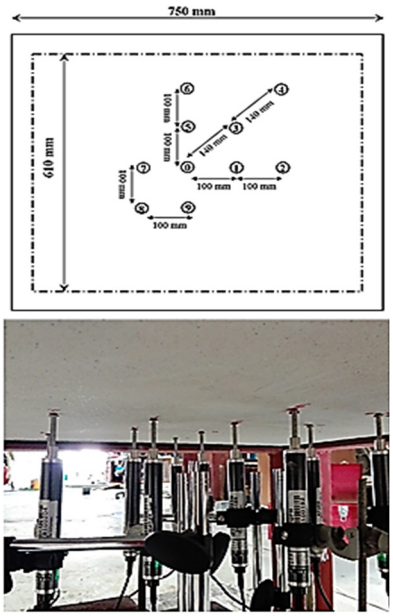

Fig. 3 LVDT locations for measuring the deflection of slab (top); LVDT's under the slab for measuring deflections (bottom)

Table 3 Loading protocols of drop weight impact test

Drop No.	Targeted cumulative impact energy (J)	Required drop height (mm)	Impact velocity (m/sec)
1	124	600	3.43
2	268	700	3.71
3	433	800	3.96
4	618	900	4.20
5	824	1000	4.43
6	1051	1100	4.65
7	1298	1200	4.85
8	1566	1300	5.05
9	1854	1400	5.24
10	2163	1500	5.42
11	2493	1600	5.60
12	2853	1750	5.86
13	3245	1900	6.11
14	3667	2050	6.34
15	4151	2350	6.79
16	4666	2500	7.00
17	5212	2650	7.21
18	5789	2800	7.41
19	6397	2950	7.61

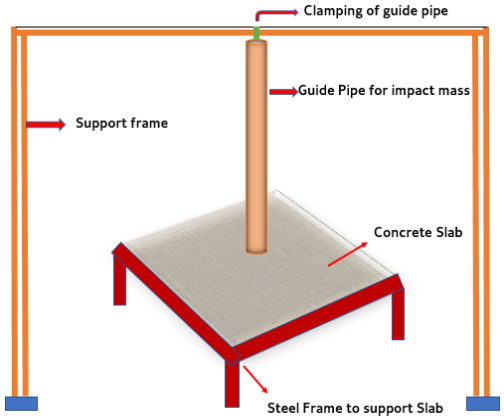

Fig. 4 Schematic diagram of the tailor-made impact test setup

Cast iron cylindrical rod (75 mm diameter, 600 mm long), weighing 21 kg, was used as an impact mass. The impactor was dropped at the center of the slab from various pre-determined heights to exert different values of impact energy. Each blow height was greater than the previous one and the test continued until the specimen showed the signs of major damage (the toughest slab specimen sustained a maximum of 19 blows). The details of drop heights and impact velocities are given in Table 3. The impact energy was calculated by using the formula of potential energy, i.e., mass ×acceleration due to gravity (9.81 m/s^2) × drop height. A steel guide pipe with holes at specified points was used to ensure the alignment of the impactor and to control the impact height. The guide pipe was clamped to a steel frame to keep it steady during the testing elevations. The schematic diagram of the impact test setup is shown in Fig. 4.

3. Results and discussions

3.1 Mechanical properties of HSCC and UHPC mixtures

The results of the mechanical properties (compressive strength, modulus of elasticity, flexural and direct tensile strengths, and fracture toughness) of the HSCC mixture without fibers and three UHPC mixtures (M-FC2, M-FC4 and M-FC6) with three different fiber contents (2%, 4% and 6% by mass), are summarized in Table 4. The 28-day compressive strengths shown in Table 4 are the equivalent cubical compressive strengths.

The variation of compressive strength with fiber content is evident from the results presented in Table 4. It can be observed that the compressive strength increased by 18% with an increase in the amount of fibers from 2 to 4%, whereas the increase in the compressive strength was only about 6% when fiber dosage was increased further from 4 to 6%. These observations match with those reported in the literature (Ahmad and Hakeem 2015, Su *et al*. 2016). Similarly, the data in Table 4 indicate that the modulus of elasticity increases by increasing the amount of fibers. However, the effect of the fiber content on the compressive strength is more than that on the modulus of elasticity. It can be noted that the modulus of elasticity increased by only 6% when fiber content was increased from 2 to 4%. An increase in the amount of fibers from 4 to 6% resulted in a very slight improvement in the modulus of elasticity (only by 3%). It shows that the resistance of the fiber is more pronounced against crushing than its resistance against axial deformation.

Table 4 Mechanical properties of the concrete mixtures tested at the age of 28 days

Mixture ID	HSCC	M-FC2	M-FC4	M-FC2
Compressive strength, f_c' (MPa)	56	132	156	166
Modulus of elasticity, E (GPa)	29.8	47.1	49.9	51.5
Flexural tensile strength, f_r (MPa)	6.14	14.04	18.48	20.95
Direct tensile strength, f_t, (MPa)	3.21	4.58	7.12	10.11
Critical stress intensity factor, K_{IC}, (MPa.$\sqrt{m}$)	0.56	1.29	1.61	2.68

In line with the compressive strength and modulus of elasticity, the flexural tensile strength of the UHPC mixtures also increased with the increase in the fiber content. However, it can be noted that the effect of the fiber content on the flexural tensile strength is relatively more significant than that on the compressive strength and modulus of elasticity. The flexural tensile strength increased by 32% with an increase in the dosage of fibers from 2 to 4% and the flexural tensile strength increased by about 14% when the dosage of fibers was further increased from 4 to 6%. The high resistance of the fiber against flexural action is because of the fact that once the concrete is cracked, fibers start taking the stresses, causing strain hardening, thus increasing the flexural capacity of the concrete. Similar observations pertaining to the influence of the dosage of fibers on the flexural tensile strength are reported in the literature (Hakeem 2011, Hakeem *et al*. 2013, Willey 2013, Li *et al*. 2016, Su *et al*. 2016). Furthermore, the effect of fiber content on the direct tensile strength (obtained from the dog-bone test) is even more pronounced. The direct tensile strength increased by 55% with an increase in the fiber content from 2 to 4% and the increase in the direct tensile strength was about 41% by increasing the amount of fibers from 4 to 6%. This is consistent with the nature of the test, where the fibers are directly active in resisting the load through the bond between fibers and the concrete matrix.

The critical stress intensity factor is used to indicate the fracture toughness of the concrete, which is the resistance of concrete against the initiation and propagation of the cracks caused by any action such as flexure or impact. Higher fracture toughness is always desirable when the concrete is supposed to be under impact due to dynamic loading or accidental loading. The fiber content of the concrete is one of the key factors that affect the fracture toughness, as evident from the results of the critical stress intensity factor measured for all three UHPC mixtures (Table 4). It can be

noted from Table 4 that the critical stress intensity factor increased by 25% by increasing the dosage of fibers from 2 to 4% and the increase in the critical stress intensity factor was 66%, with an increase in the dosage of fibers from 4 to 6%.

It is worth noting that the increase in fracture toughness with fiber content has an opposite trend as compared to the trend of increase in the other mechanical properties of the UHPC with an increase in the fiber content. The increase in compressive and tensile strengths and modulus of elasticity was higher when the amount of fibers was increased from 2 to 4% than when fiber content increased from 4 to 6%. On the other hand, the improvement in the fracture toughness was of higher magnitude by increasing the dosage of fibers from 4 to 6% as compared to that when the dosage of fibers was increased from 2 to 4%.

The HSCC mixture (without fiber) was considered along with UHPC mixtures (with different dosages of fiber) to highlight the vast difference between the basic mechanical properties and the resistance against impact of concrete without and with fibers. It can be noted that all the properties of the UHPC mixtures, as shown in Table 4, were several times better than that of the HSCC mixture. For example, the UHPC mixture containing 2% fiber (M-FC2) had compressive strength, elastic modulus, tensile strength (flexural), tensile strength (direct), and fracture toughness higher than that of the HSCC mixture by the factors of 2.4, 1.6, 2.3, 1.4, and 2.3, respectively.

3.2 Impact resistance

The surfaces of the slab specimens after subjecting them to the impact loading are shown in Fig. 5. While the slab made of HSSC (without steel fibers) failed severely under very low impact energy, the slab specimens cast using UHPC containing different amounts of steel fibers showed relatively very high degrees of resistance against impact loading. The photographs of the slabs after completing the impact test, as shown in Fig. 5, clearly indicate the significant influence of the fiber content on the development cracks under impact loading. It can be observed from Fig. 5 that the slab with 2% steel fibers exhibited a relatively more number of cracks and cracks (initiating at the central impact point) and propagating radially over larger distances as compared to the UHPC slabs with 4 and 6% steel fiber. This indicates the higher fracture toughness of the UHPC at higher fiber content (as discussed in Section 3.1) offered higher resistance against the initiation and propagation of the cracks under the impact loading.

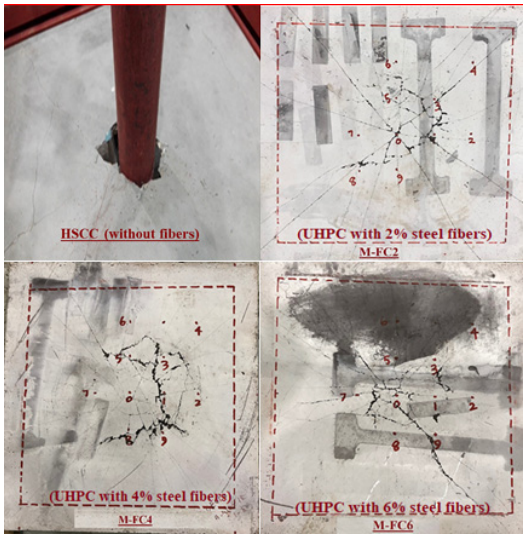

Fig. 5 Surfaces of the slabs after impact testing

The plots shown in Fig. 6 indicate the effect of the fiber content of UHPC on the impact energy absorption and central deflection of the UHPC slabs. It can be observed from Fig. 6 that with an increase in the fiber content, the energy absorption capacity is higher and the central deflection (at a particular level of the impact energy) is lower. When an energy level of 1566 J (corresponding to the 8th blow) was applied on all three slabs having different fiber contents, the central deflection in the UHPC slab containing 2% steel fibers (M-FC2) was 8.95 mm against the central deflections of 3.78 and 3.14 mm recorded for the UHPC slabs containing 4 and 6% of steel fibers (M-FC4 and M-FC6), respectively. At an impact energy level of 1566 J, while the slab M-FC2 was excessively damaged, the slab M-FC4 and M-FC6 were found without any sign of damage. Therefore, the impact test on M-FC2 slab specimen was discontinued after the 8th blow considering the maximum impact energy absorption capacity as 1566 J for the UHPC slab with 2% steel fibers. The impact test on M-FC4 and M-FC6 slabs was continued up to impact energy of 2853 J (corresponding to the 12th blow) when the M-FC4 slab was severely damaged, and at that stage, the central deflection in slab M-FC4 was recorded as 10.65 mm, which was 73% higher than that of the deflection of slab M-FC6 for the same magnitude of the impact energy (2853 J). The impact test was discontinued for the M-FC4 slab after the 12th blow considering the maximum impact energy absorption capacity as 2853 J for the UHPC slab with 4% steel fibers. Lastly, the impact test on M-FC6 slab was continued until it was severely damaged at an impact energy of 6397 J (corresponding to the 19th blow), recording a central deflection of 21.51 mm. The maximum impact energy absorption capacity for the UHPC slab with 6% steel fibers was considered as 6397 J.

It can be noted from the foregoing discussion on the experimental data pertaining to the maximum impact energy absorption capacity and central deflection of the UHPC slabs containing different percentages of steel

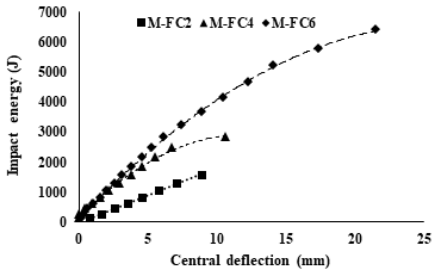

Fig. 6 Central deflection versus impact energy at the different fiber content of UHPC slab

fibers that the fiber content has a very significant influence on the impact resistance. The reason behind higher energy absorption capacity and lower central deflection at a higher fiber content in the UHPC slab can be attributed to the increase in strength, stiffness, and fracture toughness of the UHPC with an increase in its fiber content. The reason behind a very low (negligible) resistance of the HSCC slab against the impact loading as compared to the fiber-reinforced UHPC slabs is attributed to much lower strength, elasticity, and fracture toughness of HSCC with lower strength class and without steel fibers. As compared to the HSSC slab, the UHPC slab with 2% fiber content had 1.6 times higher deflection and absorbed almost two times more impact energy. The UHPC slab with 4% fiber content deflected twice more than the HSSC slab and absorbed almost six times more impact energy. The UHPC slab with 6% fiber content deflected more than five times and absorbed almost sixteen times higher impact energy as compared to the HSSC slab. It may further be noted that the impactor penetrated through the HSSC slab, as shown in Fig. 5, whereas all fiber-reinforced UHPC slabs resisted the penetration by the impactor.

3.3 Correlations of fiber content with fracture toughness of UHPC, impact energy capacity and deflection of the UHPC slab

Fig. 7 shows the effect of fiber content on the maximum impact energy absorption of the UHPC slabs. The maximum impact energy carrying capacity of the UHPC slabs improved exponentially with an increase in the amount of fibers. It can be observed from Fig. 8 that the impact energy capacity for UHPC slabs with 4% and 6% fiber content increased by 82% and 308%, respectively, as compared to the impact energy capacity of the slab cast using UHPC with 2% fiber content. This high improvement in the impact resistance by increasing the amount of fibers is due to the fact that the tensile strength and fracture toughness of the UHPC increase significantly with the increase in the fiber content, as evident from the data pertaining to the tensile strengths and fracture toughness presented in Table 4. The beneficial effect of the higher dosage of fibers on the impact resistance has been reported by several other researchers (Elavenil and Knight 2012, Kiran *et al*. 2015, Othman and Marzouk 2018, Iqbal *et al*. 2019).

Fig. 8, showing the effect of fiber content on the total central deflection of slab at failure, indicates a very significant enhancement of the central deflection of the UHPC slabs before their failure due to an increase in the fiber content. The central deflections at failure corresponding to 4 and 6% fiber contents were higher by 19 and 140%, respectively, as compared to that for the UHPC slab with 2% fiber content. This can be attributed to the fact that the fiber acts as a micro-reinforcement and slabs with higher percentages of steel fiber can undergo large deflections without disintegration due to enhancement of the ductility of UHPC with increase in the fiber content.

Fig. 9, showing the effect of the fiber content on the fracture toughness of UHPC, indicates that the impact energy absorption capacity and central deflection of the UHPC slab are mainly controlled by the fracture toughness of UHPC because the trend of the curve, as shown in Fig. 9, matches with the trends of the curves in Figs. 7 and 8 showing the effect of fiber content on impact energy absorption capacity and central deflection of the slab at failure, respectively. It can be observed from the plots shown in Figs. 7 through 9 that the enhancement in the fracture toughness of UHPC and impact resistance of the UHPC slab with increases in the fiber content from 4 to 6% is several times more than that when the amount of fibers was increased from 2 to 4 %.

The relationships of the fiber content with fracture toughness of UHPC, impact energy absorption and central deflection of UHPC slab at failure, obtained through the regression analysis, are as follows

$$K_{IC} = 0.853\ e^{0.183(FC)} \qquad (R^2 = 0.95) \tag{1}$$

$$E_u = 749\ e^{0.352(FC)} \qquad (R^2 = 0.99) \tag{2}$$

$$\Delta_u = 5.3\ e^{0.219(FC)} \qquad (R^2 = 0.89) \tag{3}$$

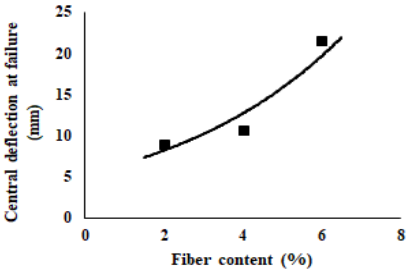

Fig. 8 Effect of fiber content on central deflection at failure of UHPC slab under impact loading

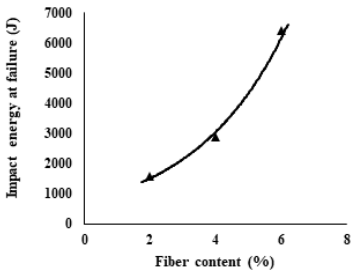

Fig. 7 Effect of fiber content on impact energy capacity of UHPC slab under impact loading

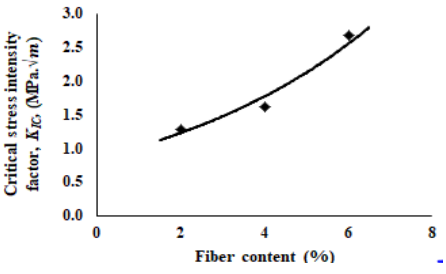

Fig. 9 Effect of fiber content on fracture toughness of UHPC

Where,

K_{IC} = fracture toughness, i.e., critical stress intensity factor (MPa.$\sqrt{\boldsymbol{m}}$)

E_u = impact energy absorption at failure (J)

Δ_u = central deflection at failure (mm)

FC = fiber content (% by mass)

Eqs. (1), (2) and (3), empirically developed using the experimental data developed under the present study, may be utilized by the mixture designer for optimizing the dosage of fibers for targeted fracture toughness, impact resistance and maximum deflection of the UHPC components having similar geometry as that of the slab specimens used in this research.

4. Finite element modeling (FEM) of slabs subjected to impact loading

The finite element modeling was conducted using ABAQUS®-Version 6.14 (Dassault Systèmes Simulia 2016). The concrete damage plasticity (CDP) model was used to define the complete behavior of UHPC mixtures. CDP model was initially introduced for monotonic loading by Lubliner (1989). Afterward, Lee and Fenves (1998) adopted it for the cyclic and dynamic loadings. The formulation of CDP is reported in the literature (Lubliner 1989, Lee and Fenves 1998, Dassault Systèmes Simulia 2016). CDP can be used to model various types of concrete by inputting the experimentally measured parameters. These parameters are well defined for normal concrete, but the performance of UHPC is a topic of research.

The input parameters of UHPC were defined using macro-level mechanical properties, based on the assumption that the steel fibers are uniformly distributed. In the CDP model, both elastic and non-linear properties were defined in the finite element model. The elastic properties were obtained from the experimental results of modulus of elasticity and Poisson's ratio of 0.2. The non-linear parameters were also extracted from the experimental curves obtained from the modulus of elasticity test and dog-bone test for uniaxial direct tension. The stiffness degradation was accounted for in the CDP model in terms of two scalar parameters (compressive and tensile damages, i.e., d_c and d_t, respectively). These damage parameters were considered as the function of plastic strains. The value of the damage parameters ranges from 0 to 1. The value of 1 means complete damage, and the value of zero means completely intact. The complete procedure for the calculation of compression damage parameters given by Birtel and Mark (2006) and for tension damage parameters given by Wahalathantri *et al*. (2011) were used.

Table 5 CDP parameters for FEM (Othman and Marzouk 2018)

Dilation angle (φ)	Plastic flow eccentricity (ϵ)	Biaxial to uniaxial compressive strengths (σ_b/σ_o) ratio	Shape factor (K_c)
36	0.1	1.16	0.667

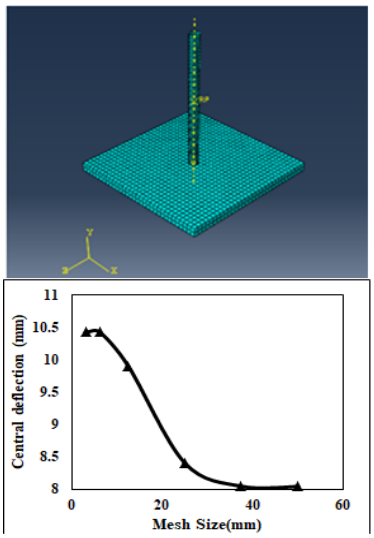

Fig. 10 FEM model (top); mesh convergence of slab (bottom)

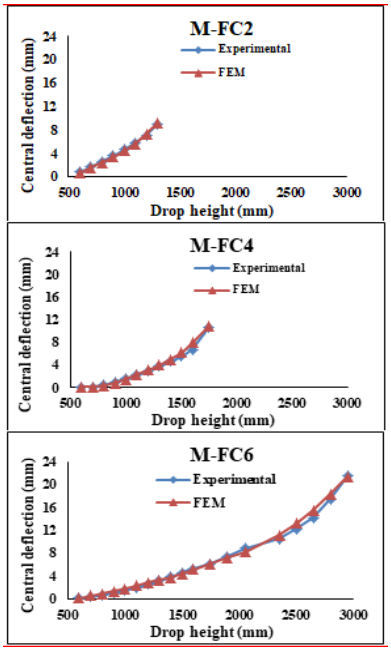

Fig. 11 Experimental versus FEM results of deflection of slabs with different fiber content

The yield surface and the flow rule were taken care of by using four parameters in the CDP. Values of these four parameters were obtained from the literature (Othman and Marzouk 2018) and shown in Table 5.

4.1 Model preparation and meshing

The size of the mesh, after performing the mesh convergence as shown in Fig. 10, was considered as 6.25 mm (8 elements across the depth of 50 mm). A time-step of 2 μs was approximately considered for the explicit analysis using the ABAQUS-Explicit. For modelling the multiple impacts by hammer, the restart-analysis option was adopted. For that, the new impact velocity of the dropping hammer

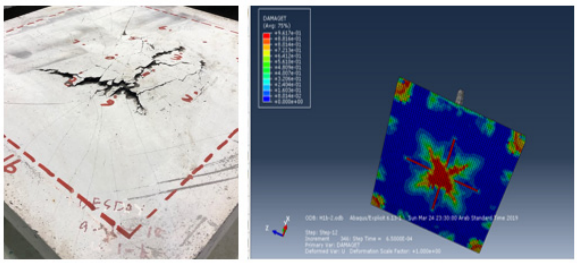

Fig. 12 Comparison of crack pattern and damage between experimental and FEM results

and the material properties from the endpoint of the preceding step was considered. This way the step-by-step effect of impact was cumulated, which mimicked exactly the way in which impact testing of slabs was carried out.

4.2 Numerical results

FEM results for the slabs with different fiber content are shown in Fig. 11. A good agreement was found between the experimental results and numerical results obtained from FEM. It is evident from Fig. 11 that the concrete damage plasticity model can be used effectively to model the behavior of UHPC slabs subjected to impact loading.

Similarly, the FEM successfully captured the crack pattern and damage evolution of the experimental test results, as shown in Fig. 12.

5. Conclusions

Based on the experimental and analytical studies carried out under the present study on examining the effect of fiber content on resistance of ultra-high performance concrete slabs against high-intensity impacts, the following conclusions were drawn:

- All the mechanical properties of the UHPC were significantly enhanced with an increase in the dosage of fibers.
- Impact resistance improved exponentially with an increase in the percentage of fibers. Like the fracture toughness of the UHPC mixture, the pronounced effect of fiber content on the resistance of the UHPC slabs against impact was observed when the percentage of fibers was increased from 4 to 6 as compared to the effect due to increase in the percentage of fibers from 2 to 4. This confirms that the fracture toughness of the UHPC mainly controlled the impact resistance of the UHPC slabs.
- Excellent correlations of fiber content with the fracture toughness of UHPC, impact energy capacity, and deflection of the UHPC slab existed as evident from the high degrees of the fits obtained for Eqs. (1) through (3).
- UHPC exhibited far superior mechanical properties than that of the HSSC. The resistance of the fiber-reinforced UHPC against impact was found far better than that of the HSSC. The UHPC slab with 6% fiber content absorbed almost sixteen times higher impact energy and deflected more than five times (before failure) as compared to the HSSC slab.
- The experimental and numerical modeling results matched very well, confirming that the concrete damage plasticity (CDP) model can effectively simulate the influence of impact loading applied to the UHPC slabs containing different fiber contents. Therefore, this model can be used for parametric study on the effect of fiber content on the resistance of UHPC slabs against impact considering various sizes of the UHPC slabs.

Acknowledgments

The authors gratefully acknowledge the support from the Civil & Environmental Engineering Department, King Fahd University of Petroleum & Minerals, Saudi Arabia.

References

Ahmad, S. and Hakeem, I. (2015), "Effect of curing, fibre content and exposures on compressive strength and elasticity of UHPC", *Adv. Cement Res.*, **27**(4), 233-239. https://doi.org/10.1680/adcr.13.00090

ASTM C150-19 (2019), Standard specification for Portland cement (pp. 1–10). West Conshohocken, PA, USA: ASTM International.

ASTM C33-18 (2019), Standard specifications for coarse aggregates (pp. 1–8). West Conshohocken, PA, USA: ASTM International.

ASTM C39-18 (2018), Standard test method for compressive strength of cylindrical concrete specimens (pp. 1–8). West Conshohocken, PA, USA: ASTM International.

ASTM C469-14 (2014), Standard test method for static modulus of elasticity and poisson's ratio of concrete (pp. 1–5). West Conshohocken, PA, USA: ASTM International.

ASTM C494-19 (2019), Standard Specification for Chemical Admixtures for Concrete (pp. 1–15). West Conshohocken, PA, USA: ASTM International.

ASTM C78-18 (2018), Standard test method for flexural strength of concrete (using simple beam with third-point loading) (pp. 1–5). West Conshohocken, PA, USA: ASTM International.

Azad, A.K., Hakeem, I. and Ahmad, S. (2012), "Effect of cyclic exposure and fibre content on tensile properties of ultra-high-performance concrete", *Adv. Cement Res.*, 1-8. https://doi.org/10.1680/adcr.12.00039

Batarlar, B. (2013), *Behavior of reinforced concrete slabs subjected to impact loads*, Izmir Institute of Technology.

Birtel, V. and Mark, P. (2006), "Numerical analyses of the biaxial shear capacity of transverse reinforced concrete members", *Proceedings of the 8th International Conference on Computational Structures Technology*, Stirling, UK.

Dadmand, B., Pourbaba, M., Sadaghian, H. and Mirmiran, A. (2020), "Effectiveness of steel fibers in ultra-high-performance fiber-reinforced concrete construction", *Adv. Concrete Constr., Int. J.*, **10**(3), 195-209. https://doi.org/10.12989/acc.2020.10.3.195

Dassault Systèmes Simulia (2016), ABAQUS 6.14. Simula, User's manual.

Elavenil, S. and Knight, G.M.S. (2012), "Impact response of plates under drop weight impact testing", *Daffodil Int. Univ. Sci. Technol.*, **7**(1), 1-11. https://doi.org/10.3329/diujst.v7i1.9580

Farnam, Y., Mohammadi, S. and Shekarchi, M. (2010),

"Experimental and numerical investigations of low velocity impact behavior of high-performance fiber-reinforced cement based composite", *Int. J. Impact Eng.*, **37**(2), 220-229. https://doi.org/10.1016/j.ijimpeng.2009.08.006

Filho, R.D.T., Koenders, E.A.B., Formagini, S. and Fairbairn, E.M.R. (2012), "Performance assessment of ultra high performance fiber reinforced cementitious composites in view of sustainability", *Mater. Des.*, **36**, 880-888. https://doi.org/10.1016/j.matdes.2011.09.022

Hakeem, I. (2011), *Characterization of ultra-high performance concrete*, King Fahd University of Petroleum and Minerals.

Hakeem, I., Azad, A.K. and Ahmad, S. (2013), "Effect of steel fibers and thermal cycles on fracture properties of ultra-high-performance concrete", *J. Test. Eval.*, **41**(3), 458-464. https://doi.org/10.1520/JTE20120182

Huang, H., Gao, X. and Khayat, K.H. (2021), "Contribution of fiber orientation to enhancing dynamic properties of UHPC under impact loading", *Cement Concrete Compos.*, **121**, p. 104108. https://doi.org/10.1016/j.cemconcomp.2021.104108

Iqbal, M.A., Kumar, V. and Mittal, A.K. (2019), "Experimental and numerical studies on the drop impact resistance of prestressed concrete plates", *Int. J. Impact Eng.*, **123**, 98-117. https://doi.org/10.1016/j.ijimpeng.2018.09.013

Kang, S.T. (2020), "The use of river sand for fine aggregate in UHPC and the effect of its particle size", *Adv. Concrete Constr., Int. J.*, **10**(5), 431-441. https://doi.org/10.12989/acc.2020.10.5.431

Kiran, T., Zai, S.A.K. and Srikant Reddy, S. (2015), "Impact test on geopolymer concrete slabs", *Int. J. Res. Eng. Technol.*, **4**(12), 110-116.

Kota, S.K., Rama, J.S. and Murthy, A.R. (2019), "Strengthening RC frames subjected to lateral load with Ultra High-Performance fiber reinforced concrete using damage plasticity model", *Earthq. Struct., Int. J.*, **17**(2), 221-232. https://doi.org/10.12989/eas.2019.17.2.221

Krishna, B.M., Reddy, V.G.P., Tadepalli, T., Kumar, P.R. and Lahir, Y. (2019), "Numerical and experimental study on flexural behavior of reinforced concrete beams: Digital image correlation approach", *Comput. Concrete, Int. J.*, **24**(6), 561-570. https://doi.org/10.12989/cac.2019.24.6.561

Lee, J. and Fenves, G.L. (1998), "Plastic-damage model for cyclic loading of concrete structures", *J. Eng. Mech.*, **124**(8), 892-900. https://doi.org/10.1061/(ASCE)0733-9399(1998)124:8(892)

Li, J., Wu, C. and Hao, H. (2015a), "Residual loading capacity of ultra-high performance concrete columns after blast loads", *Int. J. Protect. Struct.*, **6**(4), 649-669.

Li, J., Wu, C. and Hao, H. (2015b), "An experimental and numerical study of reinforced ultra-high performance concrete slabs under blast loads", *Mater. Des.*, **82**, 64-76. https://doi.org/10.1016/j.matdes.2015.05.045

Li, J., Wu, C., Hao, H., Wang, Z. and Su, Y. (2016), "Experimental investigation of ultra-high performance concrete slabs under contact explosions", *Int. J. Impact Eng.*, **93**, 62-75. https://doi.org/10.1016/j.ijimpeng.2016.02.007

Lubliner, J. (1989), "A plastic-damage model for concrete", *Int. J. Solids Struct.*, **25**(3), 299-326. https://doi.org/10.1016/0020-7683(89)90050-4

Máca, P., Sovják, R. and Konvalinka, P. (2014), "Mix design of UHPFRC and its response to projectile impact", *Int. J. Impact Eng.*, **63**, 158-163. https://doi.org/10.1016/j.ijimpeng.2013.08.003

Nuclear Energy Institute (2011), Methodolgy for performing aircraft impact assessments for new plant designs, NEI 07-13, Revision 8P.

Othman, H. and Marzouk, H. (2018), "Applicability of damage plasticity constitutive model for ultra-high performance fibre-reinforced concrete under impact loads", *Int. J. Impact Eng.*, **114**, 20-31. https://doi.org/10.1016/j.ijimpeng.2017.12.013

Raza, A. and Ahmad, A. (2020), "Reliability analysis of proposed capacity equation for predicting the behavior of steel-tube concrete columns confined with CFRP sheets", *Comput. Concrete, Int. J.*, **25**(5), 383-400. https://doi.org/10.12989/cac.2020.25.5.383

Riedel, W., Nöldgen, M., Strabburger, E., Thoma, K. and Fehling, E. (2010), "Local damage to UHPC structures caused by an impact of aircraft engine missiles", *Nuclear Eng. Des.*, **240**, 2633-2642. https://doi.org/10.1016/j.nucengdes.2010.07.036

Su, Y., Li, J., Wu, C., Wu, P. and Li, Z. (2016), "Effects of steel fibres on dynamic strength of UHPC", *Constr. Bulid. Mater.*, **114**, 708-718. https://doi.org/10.1016/j.conbuildmat.2016.04.007

Tang, C.W. (2021), "Mix design and early-age mechanical properties of ultra-high performance concrete", *Adv. Concrete Constr., Int. J.*, **11**(4), 335-345. https://doi.org/10.12989/acc.2021.11.4.335

Thai, D. and Kim, S. (2016), "Prediction of UHPFRC panels thickness subjected to aircraft engine impact", *Case Stud. Struct. Eng.*, **5**, 38-53. https://doi.org/10.1016/j.csse.2016.03.003

Wahalathantri, B.L., Thambiratnam, D.P., Chan, T.H.T. and Fawzia, S. (2011), "A material model for flexural crack simulation in reinforced concrete elements using ABAQUS", In: *The 1st International Conference on Engineering, Designing and Developing the Built Environment for Sustainable Wellbeing* pp. 260-264. Retrieved from: https://www.researchgate.net/deref/http://eprints.qut.edu.au/41712/

Willey, J.A. (2013), *Use of ultra-high performance concrete to mitigate impact and explosive threats*, Missouri University.

Yanni, V.Y.G. (2009), *Multi-Scale Investigation of Tensile Creep of UHPC for Bridge Application*, Georgia Institute of Technology.

CC